Supplementary Information

Direct Observation of Ion Distributions near Electrodes in Ionic Polymer Actuators Containing Ionic Liquids

Yang Liu, Caiyan Lu, Stephen Twigg, Mehdi Ghaffari, Junhong Lin, Nicholas Winograd, and Q. M. Zhang*

Department of Electrical Engineering, N219 MSC building, Pennsylvania State University, University Park, PA, United States 16801

Email: qxz1@psu.edu

Tel: 814-863-8994

Time of Flight-Secondary Ion Mass Spectroscopy (ToF-SIMS)

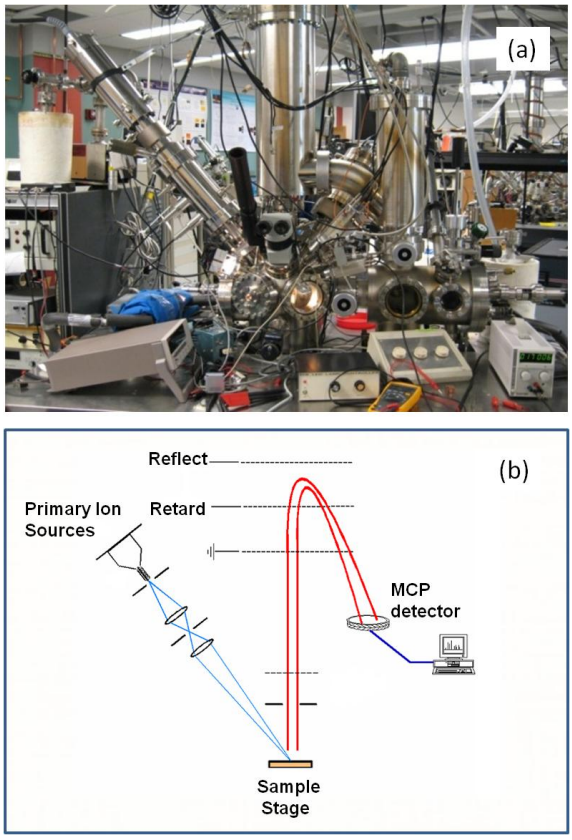

Supplementary Figure S1 (a) Picture of the ToF-SIMS served in this study. (b) Schematics of ToF-SIMS

Supplementary Figure S1(a) shows the ToF-SIMS that located in Winograd Lab at Penn State. Supplementary Figure S1(b) is the schematics of typical ToF-SIMS. High energy $C60^{+}$ Primary ions are supplied by an ion gun and focused on to the target sample, which ionizes and sputters some atoms off the surface. These secondary ions are then collected by ion lenses and filtered according to atomic mass, then projected onto an MCP detector. ToF-SIMS allows collecting data while etching into the organic materials.

Mechanical response of i-EAP actuators with ionic liquids

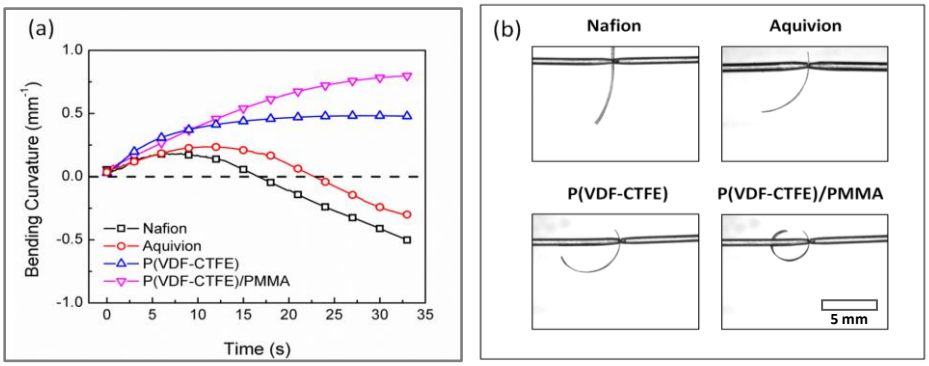

Supplementary Figure S2 (a) Time dependent bending curvature and (b) maximum bending curvature of different ionic polymer actuators with EMI-Tf electrolyte. Published in Liu, Y. et al. Macromolecules 45, 5128-5133, (2012).

Electrical and mechanical responses of Aquivion/BMMI-Cl actuator

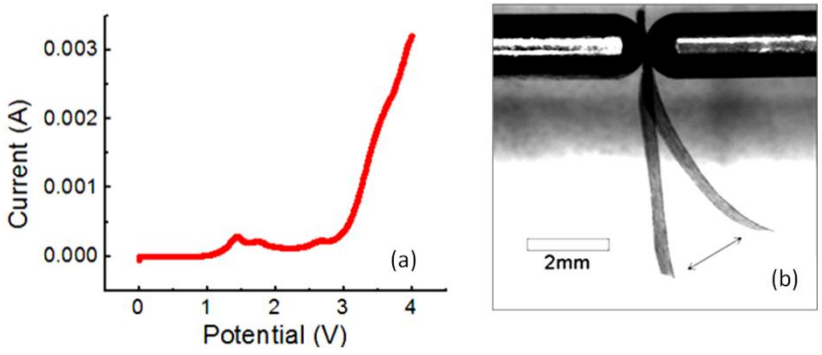

Supplementary Figure S3 (a) Linear Sweep Voltammetry at 100mV/s. (b) Bending magnitude of actuator under an AC triangular wave voltage (2.5V 0.2Hz) at 105 ℃

The electrical testing and operation voltage (2.5V) of the actuator was determined by linear sweep voltammetry in a 2-electrode device configuration, which shows the onset of the primary red-ox reaction of

the electrolytes is ~3V. Usually, for an applied voltage equal or slightly larger than the electrochemical window, one could not observe significant change in the actuation and the reaction slowly affects the bending magnitude over thousands of cycles. However, the reduction in actuator lifetime becomes notable that the actuator dies within a few minutes, when the applied voltage is a couple of volts higher than the electrochemical window.

ToF-SIMS control signal (without electrical bias)

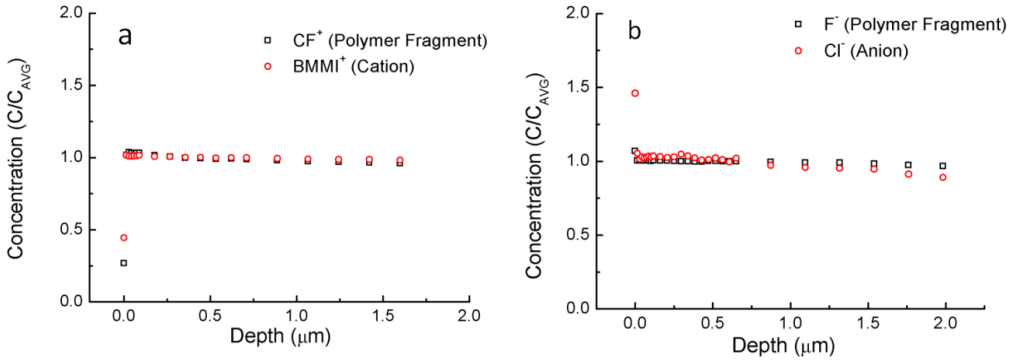

Supplementary Figure S4 Control signal of Aquivion with 45 wt% BMMI-Cl ionic liquids (a) CF^+ and $BMMI^+$ (b) F^- and Cl^- (no voltage is applied to the sample)

Control data of Aquivion with 45 wt% BMMI-Cl is presented in Supplementary Figure S4. It could be seen that without voltage bias, the counts of both the ions and polymer fragment do not change with depth. It is notable that the first data point in each data set, which represents the surface condition of the film, differs from the signal from the bulk.

Sputter rate measurement

Supplementary Table S1 Sputter rate calculated from multiple sputtering craters

Sample #	Sputter Time (s)	Depth (um)	Sputter Rate (nm/s)
dp0	1080	1.6	1.48
dp1	4740	6.41	1.35
dp2	3540	4.63	1.31
dp3	3750	6.58	1.75
dp4	4950	7.49	1.51

The average sputter rate calculated from Supplementary Table S1 is 1.48 ±0.15 nm/s.

Depth profiles of polymer fragments

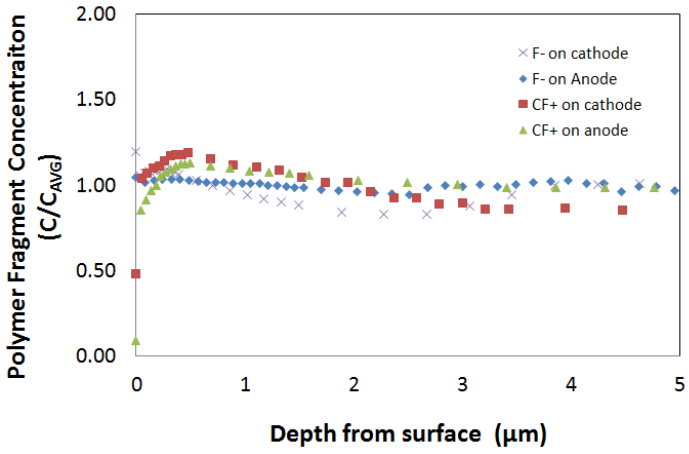

Supplementary Figure S5 Depth profile of polymer fragments under charged condition (2.5V), where the variation of the polymer signal near the electrodes is within 20%.

Ion size estimation

For the neat ionic liquid BMMI-Cl, the volume ($0.439 nm^3$) of each ion pair could be calculated from the density (0.716g/cc) and the molecular weight (188.70g/mol) of the ionic liquids. Since the size of Cl^- is well known as 181pm, from the volume of ion pair and the volume of Cl^-, the volume of BMMI and can be calculated. $BMMI^+$ and Cl^- have ion sizes (volume) 0.414 nm^3 and 0.025 nm^3, respectively.

Data analysis

a. In Figure 4(c) and (d) in main text, the curves in the surface roughness regions (d < 170 nm) may have large experimental error due to the complicated interface effects. Therefore, the curves in these narrow regions in Figure 5(a) are estimated by fittings and presented with dotted lines. The curves are fitted from the data out of roughness region (d > 170 nm) with exponential decay functions. For anions, where the data show oscillations, only the data before reaching the first minimum is used for fitting.

b. To draw Figure 5(a) from Figure 4(c) and (d) in main text, it is also necessary to find the relation between the concentrations of cation and anion in Figure 4(c) and (d). Here, charge neutrality was applied to estimate the ratio between C_0^{Ca} and C_0^{An}. By assuming the net charge on cathode side equals to that on the anode side, it is found that $C_0^{An} \sim 80\% C_0^{Ca}$, which indicates 20% of C_0^{Ca} in the entire membrane is bounded to the negatively charged side-chains of Aquivion ionomer. For

simplicity, ions attracted by the polymer side-chains are considered immobile in the consequent analysis.

Estimation of effective layer (excess ion layer) thickness

From a 5-layer model in Reference #10, the intrinsic strain S_0 generated in the effective layer (shown Supplementary Figure S6 (a)) has the following relation:

$$S_0 = -\frac{Y^m(\frac{2t^{m3}}{3} + 2t^m(t^m + \frac{t^i}{2})^2 + t^{m2}(2t^e + t^i)) + Y^e(\frac{2t^{e3}}{3} + t^e\frac{t^{i2}}{2} + t^{e2}t^i) + Y^i\frac{t^{i3}}{12}}{Y^e(t^i t^e + t^{e2})} \cdot \kappa \qquad (1)$$

where Y^m, Y^e, Y^i and t^m, t^e, t^i are the Young's modulus and the thickness of the Au metal layer, effective layer (excess ion stored), and ionic polymer layer (no strain generation), respectively. κ is the bending curvature of the actuator. Since the bending curvature in Figure 3 (c) is 0.4 mm^{-1}, strain versus effective layer thickness can be deduced as shown in Supplementary Figure S6 (b). If the intrinsic strain S_0 is 20%, which is estimated from reference # 11, the effective layers possess a thickness of 1.5 μm. If the effective layer is only in the range of nm, e. g. 5 nm, the intrinsic strain needs to reach 6000%, which is physically impossible.

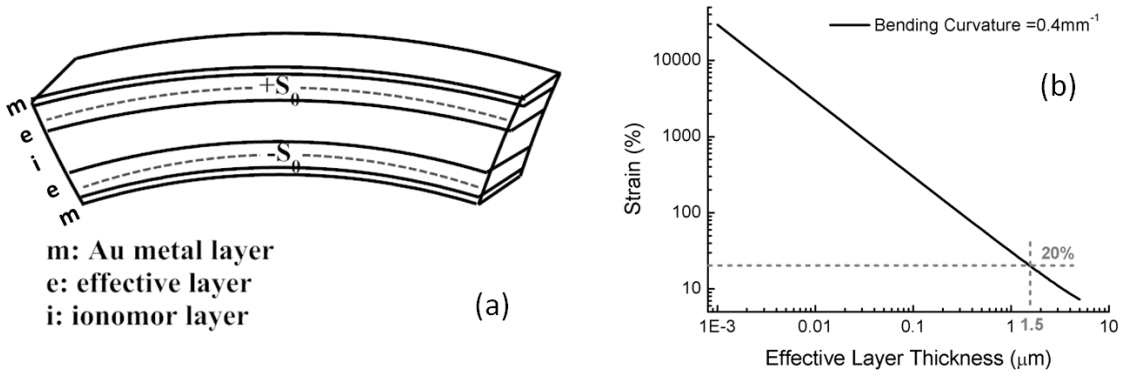

Supplementary Figure S6 (a) Schematic diagram of actuator cross-section assuming the excess ions generate $\pm S_0$ in the effective layers near two electrodes. (b) Strain versus effective layer thickness.

Illustration of ion distribution in actuator operation

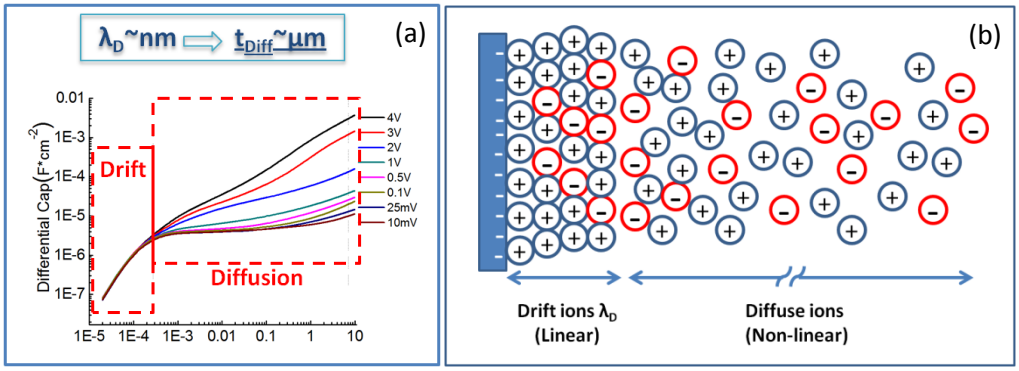

Supplementary Figure S7 (a) Differential capacitance reproduced from reference #15 (J.H. Lin et al, Polymer 2011, 52, 540-546) where step voltages are applied to ionic electroactive polymer membrane containing ionic liquids. It can be seen that drift/migration of ions is independent of voltage; however, the diffusion contribution depends on voltage, which suggests thick diffusion ion layers for higher voltages. (b) Illustration of ion distribution for ionic electroactive polymer membrane containing ionic liquids.